Short-Period Superlattice Structure of Sn-doped $In_2O_3(ZnO)_4$ and $In_2O_3(ZnO)_5$ Nanowires

Chan Woong Na, Seung Yong Bae, and Jeunghee Park
Department of Material Chemistry, Korea University

1. INTRODUCTION

The natural short-period superlattice structures have been found in the oxide compound system, such as In_2O_3-ZnO compounds that the In-O and Zn-O layer slabs stacks alternately. Since Kasper first observed the structure of $In_2O_3(ZnO)_m$ (m=2-5 and 7),[1] Kimizuka group investigated extensively the superlattice structure of homologous compounds $InMO_3(ZnO)_m$ (M = In, Fe, Ga, and Al) using high-resolution transmission electron microscopy and X-ray diffraction.[2-4]Yan et al. reported the high-resolution Z-contrast image for a modulated structure In_2O_3-ZnO.[5] As a benefit from unique crystal structure, high electrical/thermal conductivity, optical transparency, and excellent thermoelectric properties of $In_2O_3(ZnO)_5$ have been observed.[6,7] High-performance transparent field-effect transistors were fabricated using $InGaO_3(ZnO)_5$ film.[8,9]Recently, as an effort to produce the 1-dimensional nanostructures, Jie et al. synthesize the superlattice nanowires having diverse composition which is approximately $In_2O_3(ZnO)_m$ (m=5, 7, 18).[10]

2. EXPERIMENTAL DETAILS

Mixture of ZnO (99.98%, Aldrich), In (99.99%, Aldrich), and Sn (99.99%, Aldrich) powders was placed in a quartz boat located inside a quartz tube. Silicon substrate was coated with $HAuCl_4 \cdot 3H_2O$ (98%, Sigma) ethanol solution, and then positioned on the source boat. High-density nanowires were grown on the Au-deposited substrates at 900-1000 °C, by the evaporation of Zn/In/Sn source for 1 h under argon flow. As the growth temperature increases, the In/Sn content usually increases. We also synthesized pure ZnO nanowires using Zn/ZnO powder mixture at 800 °C.

3. RESULTS AND DISCUSSION

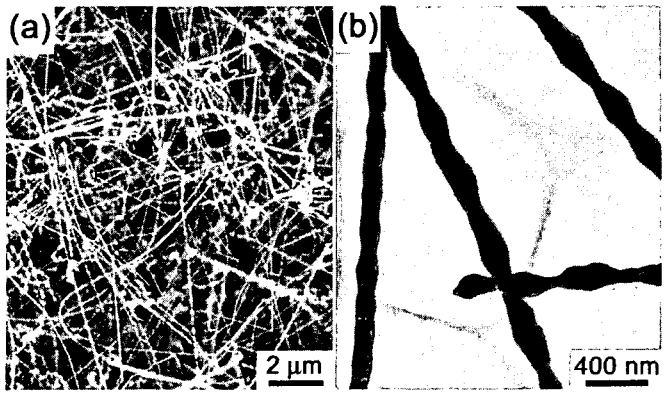

Figure 1: (a) SEM image shows Sn-doped $In_2O_3(ZnO)_5$ superlattice nanowires grown on the substrate. (b) TEM image showing a general morphology.

Figure 1(a) shows SEM image for the wire-like nanostructures grown on the substrate. The length is about 20 ㎛. Figure 1(b) corresponds to the TEM image revealing the general morphology of the nanowires that the surface is periodically bumpy. The diameter is modulated in the range of 50-90 nm. TEM image of a selected nanowire is displayed in Figure 2(a). Figure 2(b) shows high-resolution image for the tip part of this nanowire as marked in Figure 2(a). The dark lines appear periodically over the whole nanowire, with a distance of 1.9 nm. Atomic-resolved HVEM image of another nanowire taken at the [010] zone axis is displayed in Figure 2(c). Each dark line corresponds to a single plane of either In (thicker ones) or Zn atoms (thinner ones).

While the synthesis of $In_2O_3(ZnO)_5$ nanowires was carried at 900 °C, another superlattice nanowire sample has been prepared when the temperature increases to 1000 °C. The nanowires exhibit a similar morphology as that of $In_2O_3(ZnO)_5$nanowires; periodically bumpy surface due to the modulated diameter, as shown in Figure 3(a). The FFT ED pattern exhibit a series of spots emerging along the growth direction [002] of wurtzite ZnO, taken at the [2-10] zone axis [Figure 3(b)]. It corresponds to hexagonal $In_2O_3(ZnO)_4$. Figure 3(c) shows atomic-resolved HVEM image of another typical nanowire, measured at the same zone axis [2-10]. The position of In and Zn is directly determined by this image. It is seen to be mostly five layers of Zn-O slabs whose distance between the adjacent In-O layers is about 1.65 nm. The six layered Zn-O slabs appear without any periodicity and take approximately 30% of total slabs. The average composition of such polytypoid structure is close to $In_2O_3(ZnO)_4$.

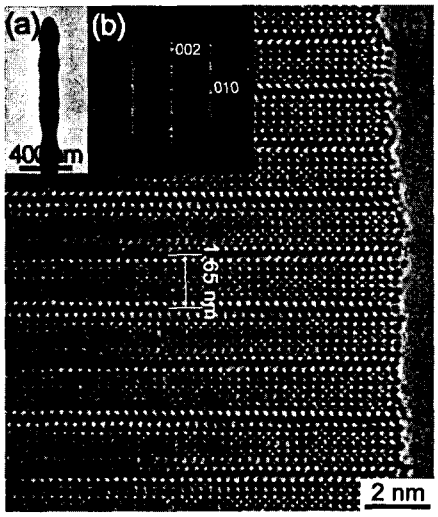

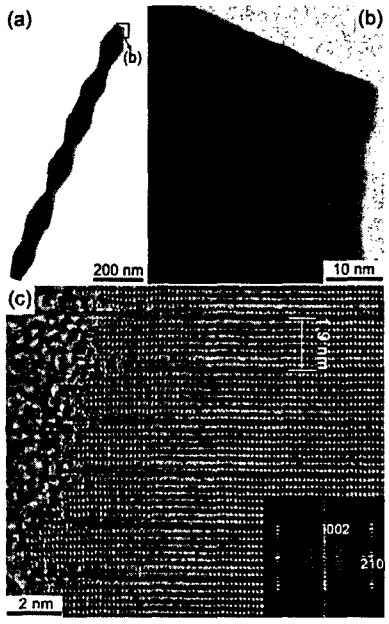

Figure 2: (a) TEM image of a selected $In_2O_3(ZnO)_5$ nanowire with corresponding (b) its atomic-resolved image.(c) HVEM image of another $In_2O_3(ZnO)_5$ nanowire with the FFT ED pattern (inset).

Figure 3: (a) TEM image of a selected $In_2O_3(ZnO)_4$ nanowire with corresponding (b) FFT ED pattern, and (c) HVEM image of another $In_2O_3(ZnO)_4$ nanowire.

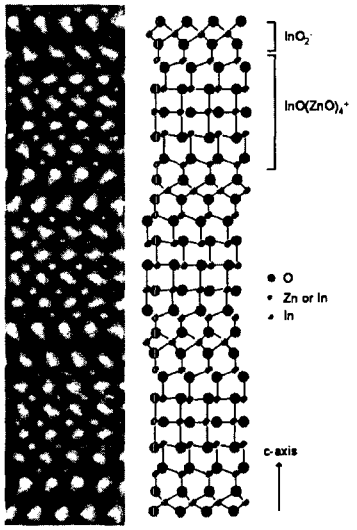

Figure 4: Atomic arrangement of $In_2O_3(ZnO)_4$ nanowires, derived from the HVEM images in the left.

Figure 4 shows a magnified HVEM image of Figure 3(c). From the TEM simulation using Java Electron Microscopy Simulation (JEMS) software, the position of Zn, In, and O atoms is drawn on the right figure. The In ions in the In-O layer occupy the octahedral sites, while In/Sn ions in the Zn-O slabs would occupy not only the tetrahedral Zn ion sites but also the trigonal/bipyramidal coordination sites.[18,22,23] We define the (001) surface as being Zn-terminated and the (00-1) surface as being O-terminated, so that the polarization is along the c-axis, the two slabs of ZnO on both sides of the In-O octahedral layer have opposite polarization. So the In-O layer inevitably induces a "head-to-head" polarization domain, so-called inversion domain boundary (IDB). Since a slab of ZnO is bounded by two IDBs, the atomic arrangement of Zn-O must be inverted. It is evidently seen that the relative position of Zn and O inside the Zn-O slabs change progressively along the growth direction (or c-axis)to produce the polarity inversion. Unlike the previous superlattice structures, the Sn element is first incorporated. The In/Sn incorporationin the Zn-O slabs may facilitate the polarity inversion inside the Zn-O slabs.

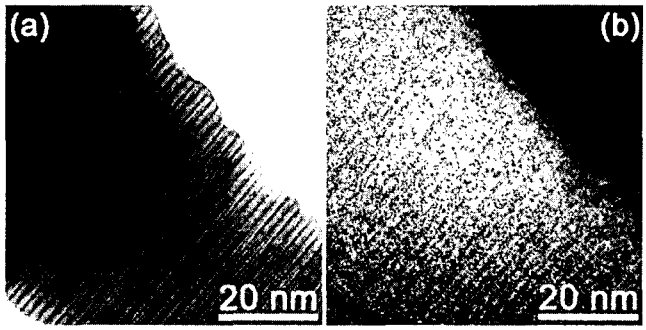

Figure 5: (a) TEM image of a selected $In_2O_3(ZnO)_4$nanowire and corresponding (b) EELS imaging of In element.

Figure 5(b) displays the EELS (or energy-filtered TEM) imaging of a $In_2O_3(ZnO)_4$ superlattice nanowire, whose corresponding TEM image is shown in Figure 5(a). Theelemental mapping of In was obtained using the electron energy loss of M-shell edges ($M_{4,5}$) (E=443.1 eV). The brighter points represent a higher concentration of the element and show that the In containing layers appear periodically along the whole nanowire. This elemental mapping confirms the alternate stacking of In-O and Zn-O slabs. The elemental mapping of Sn is not displayed, because the peaks of $M_{4,5}$ (E=484.8 eV) are nearly overlapped with that of In and so the energy filtering was not much successful.

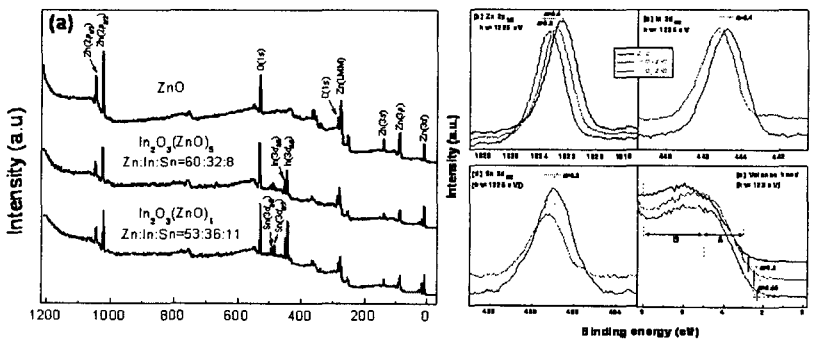

Figure 6: XPS spectrum: (a) full-range, (b) Zn $2p_{3/2}$, (c) In $3d_{5/2}$, (d) Sn $3d_{5/2}$, and (e) valence bands. The photon energy (h) is indicated in the figure.

Figure 6(a) shows a typical XPS survey scan spectrum using the photon energy 1225 eV. The XPS data shows Zn, O, In, and Sn peaks whose position is consistent with the reference.There are no

other elements except for C contaminants. The composition ratio is found to be Zn:In:Sn=60:32:8 and 53:36:11, respectively, for $In_2O_3(ZnO)_5$ and $In_2O_3(ZnO)_4$ nanowires. The finely scanned Zn $2p_{3/2}$ peak is shown in Figure 6(b). As the In/Sn content increases, the peak shifts from 1022.45 eV toward the higher binding energy, with a value of 0.40 and 0.90 eV for $In_2O_3(ZnO)_5$ and $In_2O_3(ZnO)_4$ nanowires, respectively. In contrast, the In $3d_{5/2}$ peak of $In_2O_3(ZnO)_5$ and $In_2O_3(ZnO)_4$ nanowires is located at 445.2 and 444.8 eV, showing a shift to the lower binding energy by 0.4 eV [Figure 6(c)]. The Sn $3d_{5/2}$ peak of superlattice nanowires exhibit the same behavior as that of In $3d_{5/2}$. It shifts from 487.0 eV to 487.3 eV, corresponding to the lower binding energy shift by 0.3 eV [Figure 6(d)]. These higher- and lower-energy shifts can be explained by the charge density difference between metal ions. The ion radius in the wurtzite ZnO crystal is expected to be r(Zn) = 74 pm, r(In) = 76 pm, and r(Sn) = 69 pm.[28] The respective charge is expected to be +2, +3, and +4. The higher-charge density ions In and Sn can withdraw the electrons from Zn, so the screening effect of electrons would decrease for Zn but increase for In and Sn. This implies that the incorporation of In/Sn can significantly influence the structure of valence band states.

In order to gain a deeper insight into the effect of superlattice structure on the nature of the valence bands, we obtained the valence band peaks using the photon energy 133 eV [Figure 7(e)]. The zero energy is chosen at the Fermi level, E_f, which is the threshold of the emission spectrum. The position of the valence band maximum (VBM) was evaluated by taking a linear extrapolation of the onset of valence-band emission. It shifts to the lower energy by 0.3 and 0.45 eV for the $In_2O_3(ZnO)_5$ and $In_2O_3(ZnO)_4$ nanowires, respectively. This suggests the decrease of band gap (E_g) due to the incorporation of In/Sn. For wurtzite ZnO films, the feature *A* in the energy range 3-5 eV is originated from the surface-localized O $2p$ dangling-bond states and the feature *B* in the energy range 5-8 eV corresponds to the bulk valence band originated from O $2p$ state mixed into the Zn $4sp$ and $3d$ states.

In summery, we have synthesized the Sn-doped $In_2O_3(ZnO)_4$ and $In_2O_3(ZnO)_5$ nanowires by thermal evaporation method. As the mixture of ZnO/In/Sn powders was evaporated at 900-1000 C, the nanowires were exclusively grown on the Au nanoparticles deposited silicon substrates. The diameter of nanowires is periodically modulated in the range of 50-90 nm. The HVEM and EELS imaging show unique longitudinal superlattice structure that one In-O layer and five (or six) Zn-O layer slabs stacked alternately perpendicular to the long axis, with a modulation period of 1.65 (or 1.9) nm. The Sn content is identified to be 6-8 %, which is about 1/4 of the In content, XPS. The HVEM images and FFT ED patterns reveal that the Zn-O slabs are composed of wurtzite ZnO crystals grown with the [001] growth direction, and the spacing between the In planes and its nearest Zn planes is approximately 0.3 nm which is significantly larger than the Zn (002) inter

planar spacing 0.26 nm. The atomic arrangement has been derived from the HVEM images, showing that the two slabs of ZnO on both sides of the In-O layer have opposite polarization. High-resolution XPS data suggests that In/Sn withdraw the electrons from Zn, and enhance the number of dangling-bond O 2*p* states.

4. REFERENCES

[1] Kasper, H. *Z. Anorg. Allg. Chem.* **1967**, *349*, 113.

[2] Kimizuka, N.; Isobe, M.; Nakamura, M. *J. Solid State Chem.* **1995**, *116*, 170.

[3] Li, C.; Bando, Y.; Nakamura, M.; Onoda, M.; Kimizuka, N. *J. Solid State Chem.* **1998**, *139*, 347.

[4] Li, C.; Bando, Y.; Nakamura, M.; Kimizuka, N. *Micron* **2000**, *31*, 543.

[5] Yan, Y.; Pennycook, S. J.; Dai, J.; Chang, R. P. H.; Wang, A.; Marks, T. J. *Appl. Phys. Lett.* **1998**, *73*, 2585.

[6] Hiramatsu, H.; Seo, W. S.; Kuomoto, K. *Chem. Mater.* **1998**, *10*, 3033.

[7] Masuda, Y.; Ohta, M.; Seo, W. S.; Pitschke, W.; Kuomoto, K. *J. Solid State Chem.* **2000**, *150*, 221.

[8] Nomura, K.; Ohta, H.; Ueda, K.; Kamiya, T.; Hirano, M.; Hosono, H. *Science* **2003**, *300*, 1269.

[9] Ohta, H.; Nomura, K.; Orita, M.; Hirano, M.; Ueda, K.; Suzuki, T.; Ikuhara, Y.; Hosono, H. *Adv. Funct. Mater.* **2003**, *13*, 139.

[10] Jie, J.; Wang, G.; Han, X.; Hou, J. G. *J. Phys. Chem. B* **2004**, *108*, 17027.